Revised manuscript submitted to *Measurement Science and Technology*

Curing monitoring of adhesive layers between metal adherends by ultrasonic resonance technique

Naoki Mori*, Toru Hakkaku, Takahiro Hayashi

Department of Mechanical Engineering, Graduate School of Engineering, Osaka University, Japan

* Author to whom any correspondence should be addressed.

E-mail: n.mori@mech.eng.osaka-u.ac.jp

Abstract

Layer resonance induced by ultrasonic wave incidence is applied to monitor the viscoelastic properties of a curing adhesive layer between metal plates. The theoretical analysis shows that when the adhesive layer is modeled as a linear viscoelastic material, the ultrasonic reflection spectrum takes local minima at the layer resonance frequencies depending on the wave velocity of the adhesive. On the other hand, the local minima of the reflection spectrum can be expressed as a function of the loss factor of the adhesive. Based on these results, a characterization technique for the wave velocity and the loss factor of a curing adhesive layer is proposed. This technique enables the evaluation of the viscoelastic properties even if the reflected waves from both faces of a bond layer cannot be separated. The proposed method is employed to investigate the curing behavior of bi-component epoxy adhesives. As a result, it is shown that the bonding condition affects the variation of the wave velocity and loss factor. The estimated wave velocity increases as the curing proceeds, while the loss factor sometimes takes a local maximum depending on the bonding condition and the frequency range. When the mixing ratio of the main and curing agents is imbalanced, the variation of the wave velocity becomes gradual. Furthermore, the increase in the curing temperature leads to fast changes in the wave velocity and loss factor. The proposed technique has the potential to provide insight into the curing behavior of the adhesive layer by incorporating it into other measurement methods and theories.

Keywords: Adhesive curing; Ultrasonic wave; Layer resonance; Spectral analysis; Viscoelasticity

1. Introduction

Adhesive bonding is a key technology to produce lighter and more functional structures, used in many industrial fields such as automobiles, aircraft, and electronic devices. In the bonding process, an adhesive is applied on substrate surfaces and cured by a specific reaction. For example, thermosetting adhesives are cured by elevating the surrounding temperature. Room-temperature curing structural adhesives usually consist of main and curing agents, which are mixed to induce chemical reactions without external heating. Since the material properties of an adhesive including mechanical strength and stiffness depend sensitively on its curing state, monitoring of adhesive curing reactions gains attention in the fields of not only material science but also manufacturing.

Ultrasonic waves are known as a means of nondestructive evaluation (NDE) for various structures and can be applied to characterize polymer materials and adhesively bonded joints [1]–[5]. Ultrasonic propagation characteristics in a material, e.g., the wave velocity and the attenuation coefficient, are theoretically related to its viscoelastic properties. Namely, the measurement of ultrasonic responses enables the monitoring for the mechanical properties of the material [6]–[11], which were used to examine glass transition and relaxation phenomena [12]–[19]. Matsukawa and Nagai [15] measured ultrasonic transmission in polymerizing epoxy resins and examined the effect of imbalanced curing agents on the wave velocity and attenuation coefficient, which was discussed by comparing to glass transition temperatures. Dixon and co-workers [9] developed a non-contact ultrasonic measurement system with electromagnetic transducers (EMATs) and revealed the changes in the velocity and attenuation coefficient of the shear wave with the curing time of epoxy adhesives. More recently, Adachi and co-workers [20] have focused on the availability of a spring-type interface model to ultrasonic wave propagation in a thin adhesive layer between adherends, showing the relation between the curing progress and the interfacial stiffness and discussing the limitations of the theoretical model.

However, to the authors' knowledge, previous studies regarding the ultrasonic monitoring of resin curing have considered either thick or thin bond layer and have required the adherends to be sufficiently thick to differentiate the wave packets from the interlayer. In the former case, e.g., a bond layer with a thickness of larger than 1 mm, the direct wave and round-trip components from the bond layer can be separated by setting appropriate time gates in the measured waveforms [6]–[19] if an incident ultrasonic pulse has a sufficiently high frequency. The extracted wave packets provide the wave velocity and attenuation coefficient, which reflect on the curing state of the adhesive. For thin bond layers, e.g., layers with thicknesses of a few tens of micrometers, the direct wave and round-trip components are overlapped and not separable in the temporal waveforms. Accordingly, the reflection or transmission coefficient is measured instead [20],[21]. If the adhesive layer is sufficiently thin compared to the wavelength of the incident wave, the

amplitude of the reflection (transmission) coefficient decreases (increases) monotonically with the layer stiffness, which is related to the viscoelastic properties and layer thickness. On the other hand, curing monitoring techniques for adhesive layers with intermediate thicknesses, namely, when the bond thickness is comparable to the ultrasonic wavelength and the direct wave and round-trip components are inseparable, have not been explored in detail in previous studies. For such adhesive layers, evaluating the viscoelastic properties is not straightforward compared to the two cases mentioned above. Since the bond layer thickness could affect the curing behavior of the adhesive, it may be meaningful to provide ultrasonic monitoring methods coping with various scales of adhesive thicknesses.

The present study aims to propose an ultrasonic monitoring technique for the viscoelastic characterization of curing adhesive layers between metal adherends. Based on the theoretical aspects of layer resonance characteristics, this technique enables the evaluation of the viscoelastic properties even if the reflected waves from both faces of a bond layer are inseparable. The resonance characteristics of an adhesive layer are theoretically derived and applied to the signal processing for the measured waveforms. The proposed method is used to examine the curing behavior of two different room temperature curing adhesives by evaluating their viscoelastic properties.

This paper is organized as follows. In Section 2, specimens and experimental setup are described. Subsequently, theoretical models and formulation are explained and applied in the proposal of the ultrasonic characterization technique in Section 3. The measured results are shown in Section 4, where the effects of the curing agent and the curing temperature on the curing behavior are discussed.

2. Experiment

2.1 Specimens

In this study, curing processes are investigated for single lap adhesively bonded joints. As shown in Fig. 1, aluminum alloy 5052 plates were used as adherends, whose length and width are 100 mm and 20 mm, respectively. The thickness of the adherends was $h_0 = 2.0$ mm. Two carbon steel plates with a length of 80 mm, a width of 20 mm, and a thickness of $H = 2.2$ mm were used as shim and spacer. The former and latter play roles in setting the bond length L and the bond thickness h, respectively. Namely, the bond thickness was expected to be $h \approx 0.2$ mm, and the overlap length to be $L = 20$ mm.

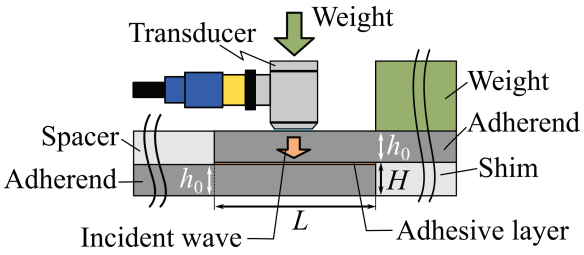

Fig. 1 Schematic of specimen and measurement setup.

Two types of adhesives were used to produce bonded joints. Adhesive 1 is commercially available as a ThreeBond epoxy adhesive 2082C, consisting of main and curing agents. In this study, the mixing ratio α is defined as the amount of the curing agent divided by that of the main agent. For properly adhesive curing, Adhesive 1 requires the mixing ratio to be $\alpha = 1$. Adhesive 2 is also a bi-component epoxy adhesive (DP420, 3M) with a mixing ratio of $\alpha = 1/2$, which was controlled by using a mixing nozzle. Table 1 gives the curing properties of the two adhesives extracted from the datasheets. At around a temperature of $T = 25$ ℃, the pot lives of Adhesives 1 and 2 are 70 min and 20 min, respectively, and their final curing times are 24 h. Each adhesive was cured under different conditions to examine the ultrasonic responses and the material properties.

Table 1 Mixing ratio, pot life, and curing time of adhesives extracted from datasheets

	Mixing ratio α	Pot life	Final curing time
Adhesive 1 (2082C)	1	70 min (25 ℃)	24 h (25 ℃)
Adhesive 2 (DP420)	1/2	20 min (24 ℃)	24 h (24 ℃)

2.2 Measurement procedures

Pulse-echo measurements were performed for single lap joints described in the previous section. After setting adherends and applying an adhesive, an Olympus piezoelectric transducer V116-RM with a nominal frequency of 20 MHz and an element diameter of 3 mm was attached to the center of the joint surface via an acoustic couplant (B2, Olympus). A pulse voltage was supplied to the transducer by a pulser/receiver (DPR300, JSR Ultrasonics) to emit a longitudinal wave, and the reflected waves were detected by the same transducer. The received signals were passed in the pulser/receiver, and the reflection waveform was recorded by a Tektronix oscilloscope MDO3014 after averaging over 64 synchronized signals. The obtained data were sent to a PC via LabVIEW.

The reflection waveform from the adhesive layer was extracted and analyzed by fast Fourier transform (FFT) to calculate the amplitude spectrum $A_R(f)$, where f is frequency. Additionally, for

a single adherend, a reflected wave from its bottom surface was measured to obtain the reference waveform, which provides the incident spectrum $I(f)$. The reflection spectrum for the adhesive layer was calculated by

$$|R| = \frac{A_R(f)}{I(f)}, \tag{1}$$

which depends on frequency.

Each adhesive was cured in an incubator (IC101W, Yamato Scientific Co., Ltd.) to control the temperature. Adhesive 1 was cured at a temperature of T = 25 ℃ with three different mixing ratios of the curing and main agents, α = 1, 1/2, and 1/3. It is repeated here that α = 1 is the appropriate mixing ratio for Adhesive 1. The curing of Adhesive 2 was carried out at a fixed mixing ratio α = 1/2 under three different temperatures, i.e., T = 20 ℃, 30 ℃, and 40 ℃.

After mixing the main and curing agents, the ultrasonic measurement began in a few minutes. When the first waveform was acquired was set as $t_E = 0$, where t_E denotes the elapsed time. In all bonding conditions, an ultrasonic response was measured every three minutes (0.05 hour) during $0 < t_E < 24$ h. Finally, the thicknesses of the overlap part and the two adherends were measured with a micrometer gauge to obtain the bond thickness h.

3. Theory

3.1 Theoretical model

To establish the evaluation principle for curing adhesive layers, the theoretical modeling is presented in this section. Fig. 2 shows the theoretical model of an adhesive joint considered in this study. The x axis represents the thickness direction of the joint. A planar adhesive layer with a thickness of h, i.e., $0 < x < h$, couples two semi-infinite adherends $x < 0$ and $x > h$. The adhesive and adherends are assumed to be homogeneous and isotropic. In this study, the effects of adhesive interfaces are not taken into consideration. Different models for adhesive joints are shown in detail in Ref. [22].

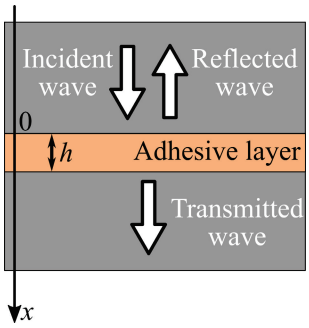

Fig. 2 Theoretical model of an adhesive layer between semi-infinite adherends subjected to normal incidence of a longitudinal wave.

When a longitudinal plane wave, whose displacement component is given by $u = u(x, t)$ with time t, is normally incident on the adhesive layer from $x < 0$, the wave propagation behavior is substantially one-dimensional. If the displacement component is expressed in the frequency domain, i.e., $u = U(x, \omega)\exp(-\mathrm{i}\omega t)$, where $\mathrm{i} = \sqrt{-1}$ and ω is angular frequency, the equation of motion leads to

$$-\rho\omega^2 U = \frac{\partial \Sigma}{\partial x}, \tag{2}$$

where $\Sigma(x, \omega)$ is the frequency-domain representation of normal stress σ, and ρ is mass density depending on materials.

Adhesive and adherend materials are modeled as linear viscoelastic bodies with complex elastic coefficients $C - \mathrm{i}D$, i.e.,

$$\sigma = (C - \mathrm{i}D)\varepsilon = \rho c^2(1 - \mathrm{i}\zeta)\varepsilon, \tag{3}$$

where ε is normal strain, c is wave velocity, and ζ is loss factor [23]. In this study, the adherends are assumed to be purely elastic, i.e., $\zeta = 0$, while the adhesive has nonzero loss factor $\zeta > 0$. The complex wave velocities of adherends and adhesive are expressed as

$$v_0 = c_0, \qquad v = c\sqrt{1 - \mathrm{i}\zeta}, \tag{4}$$

respectively. In this study, the wave velocity c and loss factor ζ of the curing adhesive are estimated by monitoring its responses to the ultrasonic wave incidence.

3.2 Ultrasonic reflection spectrum and layer resonance

The formulation in the previous section leads to the derivation of the amplitude reflection spectrum

$$|R| = \left| \frac{-1 + \exp(2\mathrm{i}\phi)}{1 - r^2 \exp(2\mathrm{i}\phi)} r \right|, \tag{5}$$

in the stress component from the adhesive layer [23]–[25], where $r = (z_0 - z)/(z_0 + z)$ is the reflection coefficient between adherend and adhesive, $z_0 = \rho_0 v_0$ and $z = \rho v$ are the acoustic impedances of adherend and adhesive, respectively, and $\phi = \omega h/v$. It is noted that the reflection coefficient r is complex and expressed as $r = s\exp(\mathrm{i}\theta)$, where $0 \le s \le 1$ and $0 \le \theta < 2\pi$. In this study, the magnitude of the acoustic impedances is assumed to satisfy $|z_0| > |z|$ because the adhesive layer sandwiched by metal adherends is of interest. The quantity $\phi = p - \mathrm{i}q$ is also complex, their real and imaginary parts given by

$$\begin{aligned} p &= \frac{\omega h}{c}\,\mathrm{Re}\left(\frac{1}{\sqrt{1 - \mathrm{i}\zeta}}\right) \cong \frac{\omega h}{c}\left(1 - \frac{3}{8}\zeta^2\right), \\ q &= \frac{\omega h}{c}\,\mathrm{Im}\left(\frac{1}{\sqrt{1 - \mathrm{i}\zeta}}\right) \cong \frac{\omega h}{2c}\zeta, \end{aligned} \tag{6}$$

where the approximation holds at sufficiently low loss factors $|\zeta| \ll 1$. Based on this notation, the energy reflection spectrum $\eta = |R|^2$ is obtained as

$$\eta = \frac{s^2\{1-\exp(-2q)\}^2 + 4s^2\exp(-2q)\sin^2 p}{\{1-s^2\exp(-2q)\}^2 + 4s^2\exp(-2q)\sin^2(p+\theta)}. \tag{7}$$

If the frequency dependences of s, θ, and $\exp(-2q)$ are weak, the reflection spectrum $|R|$ takes local minima at $\sin^2 p = 0$ [23]–[25], i.e.,

$$p = p_m = m\pi, \tag{8}$$

where $m = 1, 2, \ldots$, and the local minimum of the energy reflection spectrum η_m is given by

$$\eta = \eta_m = \frac{s^2\{1-\exp(-2q_m)\}^2}{\{1-s^2\exp(-2q_m)\}^2 + 4s^2\exp(-2q_m)\sin^2\theta}, \tag{9}$$

where $q = q_m$ is calculated by using $p = p_m$.

3.3 Characterization procedure of adhesive layer

The reflection spectrum $|R|$ measured for the adhesive layer provides two types of quantities that characterize the layer resonance phenomenon. Fig. 3(a) shows the theoretical reflection spectra calculated for a few conditions by Eq. (5). In this figure, the wave velocities were set as c = 1.6 km/s and 2.6 km/s at a fixed loss factor of $\zeta = 0.1$, where the thickness and mass density of the adhesive were fixed at h = 0.2 mm and $\rho = 1.20 \times 10^3$ kg/m^3, respectively. Each reflection spectrum takes local minima at multiple frequencies, which depend on the wave velocity c. These frequencies correspond to the resonance condition given by Eq. (8). More specifically, if a resonance frequency f_m is identified in the reflection spectrum, the wave velocity of the adhesive is estimated as

$$c = \frac{2hf_m}{m}, \tag{10}$$

where the bond thickness is assumed to be known *a priori*. The estimation procedure in the proposed technique is schematically shown in Fig. 4. Equation (10) is based on Eq. (6) when neglecting the second-order term regarding the loss factor ζ. As shown later in the experimental results, this assumption is valid because the loss factor of the adhesives used in this study was lower than 0.3. Namely, if the second-order term is strictly considered in the evaluation, its effect is lower than $3\zeta^2/8 < 0.03 \approx 3$ %. This approximation does not greatly affect the results in the present paper. The effect of the loss factor on the resonance frequencies is also insignificant for the metal-plastic bilayer laminates [25]. It is noted that the wave velocity is obtained for every resonance frequency f_m by Eq. (10).

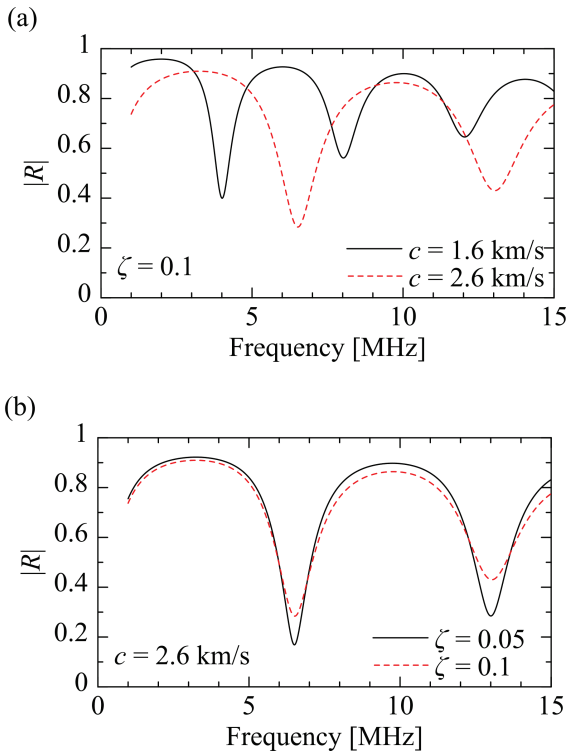

Fig. 3 Theoretical reflection spectra for different bond properties at a fixed bond thickness of h = 0.2 mm, calculated for (a) two different wave velocities at a fixed loss factor of ζ = 0.1 and (b) two different loss factors at a fixed wave velocity of c = 2.6 km/s.

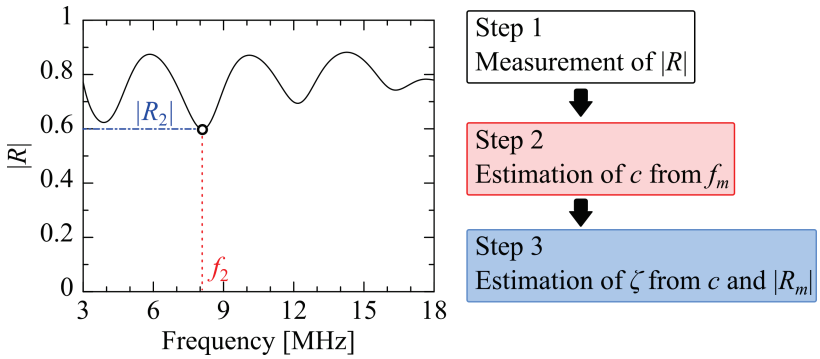

Fig. 4 Estimation procedure of the wave velocity c and loss factor ζ in the proposed technique. Steps 1–3 are repeated for every waveform.

The loss factor of the adhesive ζ can be related to a local minimum in the reflection spectrum. Fig. 3(b) shows the reflection spectra calculated for two loss factors ζ = 0.05 and 0.1 at a fixed wave velocity of c = 2.6 km/s, where the thickness and mass density of the adhesive were the same as the ones in Fig. 3(a). The resonance frequencies are unchanged if the loss factor ζ changes, while the local minima of the reflection spectrum depend on ζ. This feature is used to estimate

the loss factor ζ. If the local minimum of the reflection spectrum for a resonance frequency f_m are measured as $|R_m|$, the loss factor ζ can be obtained by solving the following equation

$$F_m(\zeta) = \frac{\{1 - \exp(-2q_m)\}^2}{\{1 - s^2 \exp(-2q_m)\}^2 + 4s^2 \exp(-2q_m) \sin^2 \theta} = \left(\frac{|R_m|}{s}\right)^2, \quad (11)$$

which is based on Eq. (9) with the wave velocity of the adhesive c given by Eq. (10). Similarly to the wave velocity, the loss factor is obtained for every resonance frequency f_m. Since the function on the left-hand side of Eq. (11) satisfies $0 < F_m(\zeta) < 1$, $F_m(0) = 0$, and $F_m(\zeta) \to 1$ at $\zeta \to \infty$, at least one solution $\zeta = \zeta_m > 0$ exists if $|R_m|/s < 1$. In this study, the bisection method was used to numerically solve Eq. (11), whose real solution was obtained as the estimated loss factor ζ.

In the proposed technique of this study, the effects of the interfaces between adhesive and adherend are not considered. Characterizing adhesive interfaces would be essential to guarantee the integrity of adhesive joints, which remains a future study. Furthermore, the proposed method is applicable to bond layers whose thickness is comparable to the ultrasonic wavelength but is not suitable for extremely thick bond layers. It would be necessary to use different characterization techniques depending on the thickness of bond layers.

4. Results and discussions

4.1 Monitoring of ultrasonic responses

The reference waveform measured for a single adherend is first shown in Fig. 5(a). The rapid change before the time $t = 0.5$ μs corresponds to the voltage supply into the transducer. The wave packet at around $t = 0.8$ μs corresponds to the bottom echo from the adherend surface, which is used to calculate the incident spectrum $I(f)$ in Eq. (1). The waveform was extracted by multiplying a turkey window, which consists of flat and tapered parts. The gate range shown in Fig. 5(a) represents the flat part, and the window decreases smoothly to zero in 0.2 μs following a cosine function. The wave packet observed at around $t = 1.4$ μs corresponds to the round-trip component in the single plate, which was excluded in the calculation of the incident spectrum $I(f)$ by FFT.

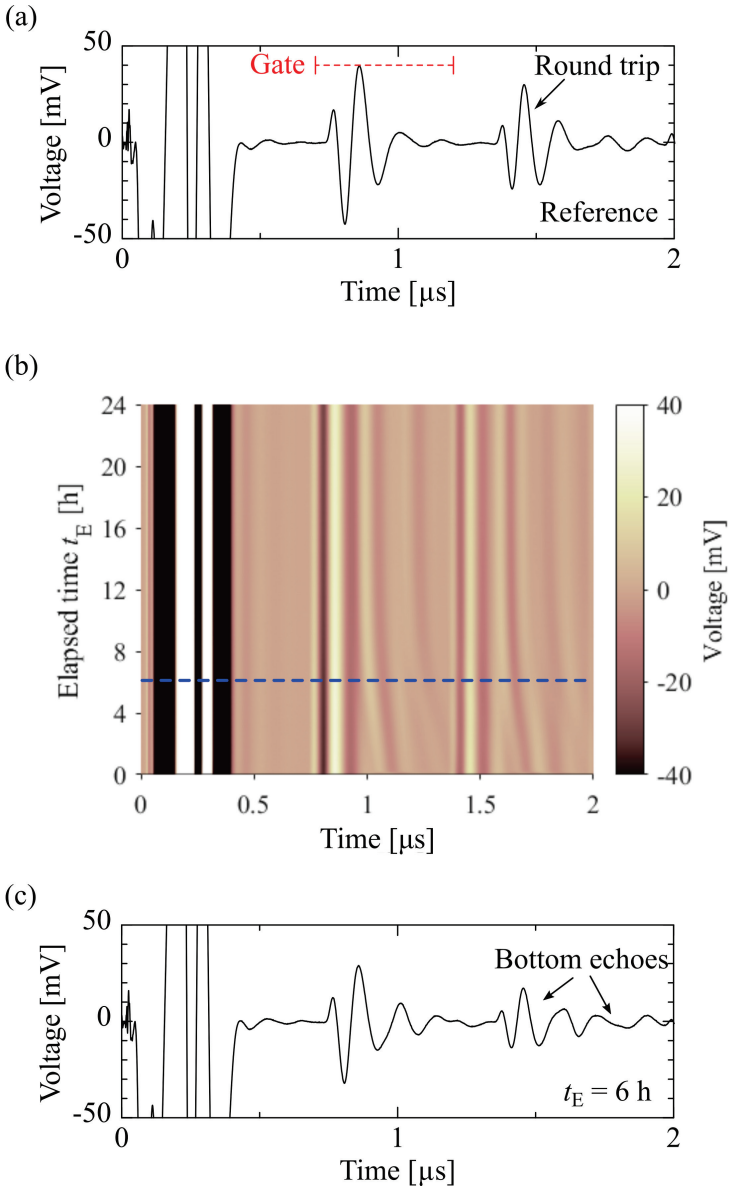

Fig. 5 (a) Reference waveform obtained for a single adherend and (b) variation of measured waveforms for a curing adhesive joint. Adhesive 1 (2082C) with the mixing ratio $\alpha = 1$ was cured under a temperature of $T = 25$ °C. A horizontal dashed line in (b) represents the elapsed time of $t_E = 6$ h, at which the corresponding waveform is shown in (c).

The monitoring of ultrasonic responses was performed for Adhesive 1 (2082C) with the mixing ratio of $\alpha = 1$ under the temperature of $T = 25$ °C. Fig. 5(b) shows the variation of the waveform measured for the curing adhesive joint with the elapsed time t_E. The horizontal dashed line in Fig. 5(b) represents the elapsed time of $t_E = 6$ h, at which the corresponding waveform is shown in Fig. 5(c). Compared to the reference waveform in Fig. 5(a), the amplitude of the first wave packet at around $t = 0.8$ μs is slightly low. This difference results from the adhesive layer

sandwiched between two adherends. The tail of the waveform after t = 1.0 μs seems to contain reflected wave components from the adhesive layer, but they are not separable in the time domain. The measured waveform at each elapsed time t_E was extracted using the same window function as the one for the reference waveform to calculate the amplitude spectrum by FFT.

The amplitude spectra calculated for the reference waveform and the waveforms measured at several elapsed times t_E are shown in Fig. 6(a). The reference spectrum has a center frequency of approximately 7.5 MHz, showing steep and gradual distributions in lower and higher frequency ranges, respectively. This result would reflect the fact that the transducer used in the present experiment has a nominal frequency of 20 MHz, but high-frequency components exhibit relatively severe attenuation. The amplitude spectra measured for a curing adhesive joint take several local minima at different frequencies, which are not observed in the reference spectrum.

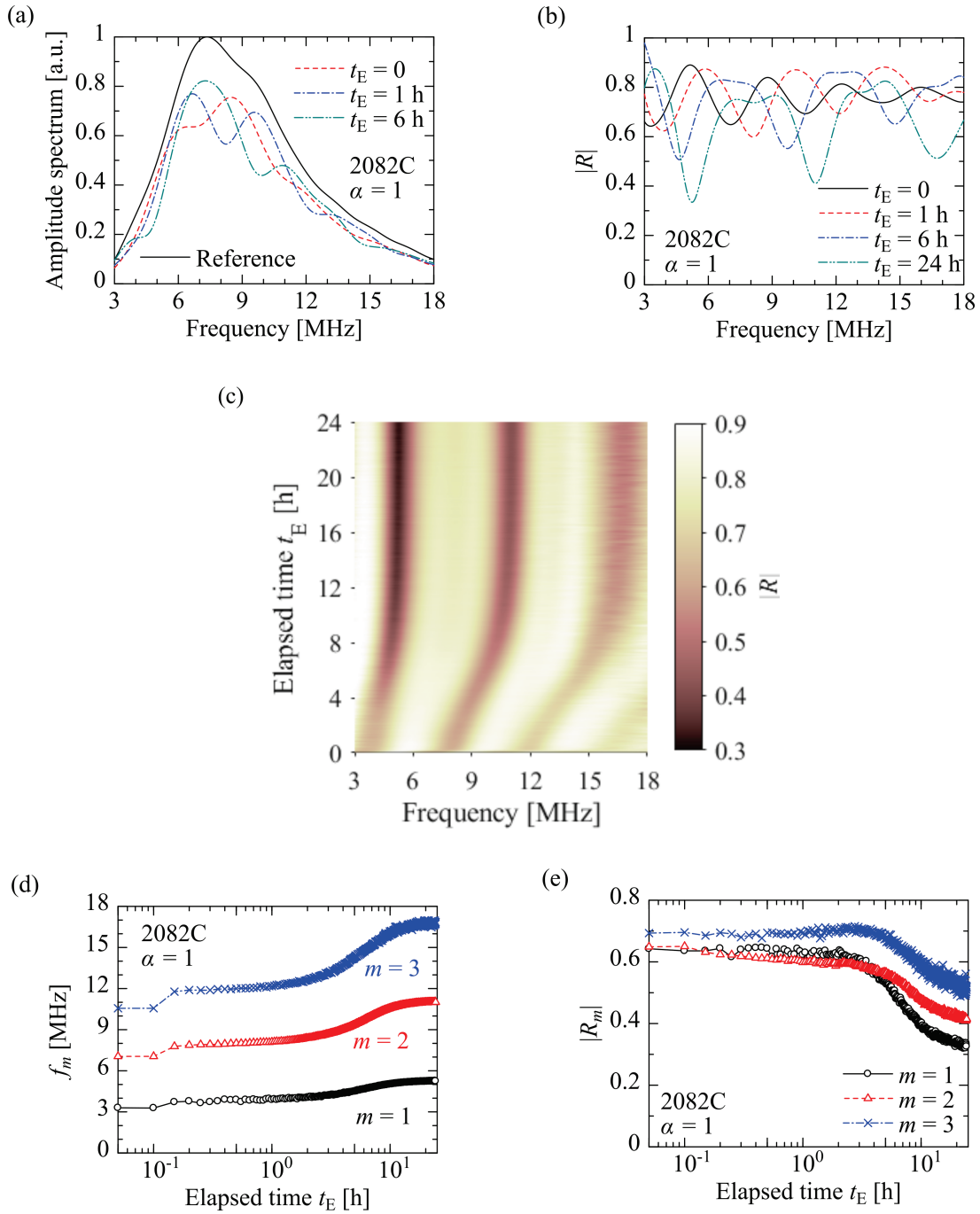

Fig. 6 (a) Amplitude spectra calculated from the reference waveform and the waveforms measured at several elapsed times t_E and (b) the resulting reflection spectra $|R|$, obtained for Adhesive 1 with the mixing ratio α = 1. The variation of the reflection spectrum $|R|$ with the elapsed time t_E is given in (c). (d) and (e) show the variation of the resonance frequencies f_m and the local minima $|R_m|$ with the elapsed time, respectively, which are extracted from (c).

Fig. 6(b) shows the reflection spectra $|R|$ calculated for several elapsed times t_E by Eq. (1). It is confirmed that multiple local minima appear at different frequencies, which change with the elapsed time t_E. These frequencies correspond to the resonance frequencies of the adhesive layer. The variation of the reflection spectrum $|R|$ with the elapsed time t_E is shown in Fig. 6(c). The resonance frequencies f_m and local minima $|R_m|$ are extracted from this figure and plotted in Fig. 6(d) and (e), respectively. In both figures, the index m represents the order of the resonance mode. After starting the measurements at $t_E = 0$, the three resonance frequencies f_1–f_3 in Fig. 6(d) increase monotonically and converge around at t_E = 24 h. For example, the resonance frequency f_2 was measured to be 11.02 MHz at t_E = 24 h, having reached its 90 percent (10.91 MHz) at approximately t_E = 15 h. On the other hand, in Fig. 6(e), the local minima $|R_1|$–$|R_3|$ measured at t_E = 24 h are lower than the ones at t_E = 0, but their variation in $0 < t_E < 24$ h is not necessarily monotonic. The 2nd-order local minimum $|R_2|$ shows monotonically decreasing behavior, while the 3rd-order local minimum $|R_3|$ has a broad peak at around t_E = 3 h. Nevertheless, in either case, their changes become gradual around t_E = 16 h.

Substitution of the resonance frequencies f_m and the local minima $|R_m|$ into Eqs. (10) and (11) leads to the estimation of the wave velocity c and the loss factor ζ, respectively. Fig. 7(a) shows the variation of the wave velocity c with the elapsed time t_E, calculated for the resonance orders of m = 1–3. The lines in this figure represent the moving averages of neighboring five points. The wave velocities in Fig. 7(a) show monotonically increasing trends with the elapsed time. The difference between the wave velocities estimated from the resonance frequencies f_2 and f_3 are relatively slight, while the estimated result by the resonance frequency f_1 is lower than the other two. Previous studies [6]–[19] reported that the wave velocity of polymer materials increases as the polymerization proceeds and often shows frequency dependence. The results in Fig. 7(a) imply that Adhesive 1 shows a similar trend, which is further considered in the next section.

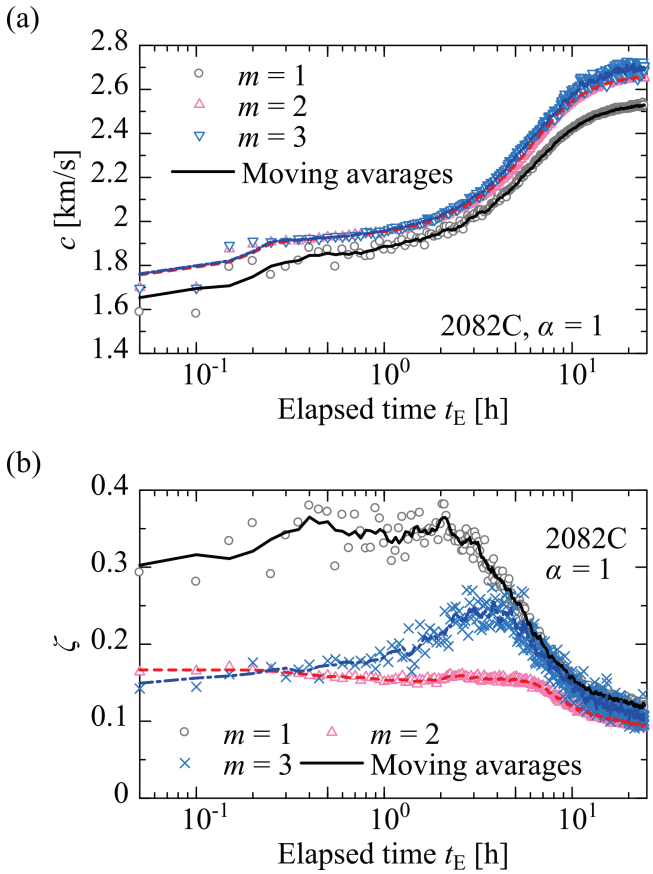

Fig. 7 Variation of (a) the wave velocities and (b) the loss factors of Adhesive 1 at the mixing ratio α = 1 with the elapsed time t_E, estimated from the resonance frequencies and local minima at the orders m = 1, 2, and 3, respectively. The lines represent the moving averages of neighboring five points.

The variation of the loss factor ζ with the elapsed time t_E is shown in Fig. 7(b) for the resonance orders of m = 1–3. The estimated results have fluctuations, but the loss factors obtained for m = 1, 2, and 3 show trends to have a peak at around t_E = 2 h, 2.5 h, and 4 h, respectively. Previous studies reported that the frequency dependence of the wave attenuation coefficient is more significant than that of the phase velocity [9], and a peak of the wave attenuation coefficient can appear during the polymerization process [6],[8],[12],[13],[15],[16]. This feature is in qualitative agreement with the results in Fig. 7(b). The frequency dependence is apparent in the initial range of the elapsed time but becomes less significant around t_E = 24 h. Freemantle and Challis [16] inferred that the attenuation coefficient initially increases because of the formation of the polymer chains and the increase in the degree of freedom and then decreases because the cross-linking begins to prevent the polymer chains from moving.

The estimated wave velocity and loss factor of the adhesive yield the theoretical reflection spectrum. Fig. 8(a)–(d) show the comparison of the measured and estimated reflection spectra at

four elapsed times t_E = 0 h, 1 h, 6 h, and 24 h, respectively. The theoretical reflection spectra in these figures were calculated by using the wave velocity and loss factor estimated by the 2nd-order resonance frequency f_2 and local minimum $|R_2|$. This estimation is based on the single resonance, but the trends of the measured reflection spectra are well reproduced in the entire frequency range by the estimated results.

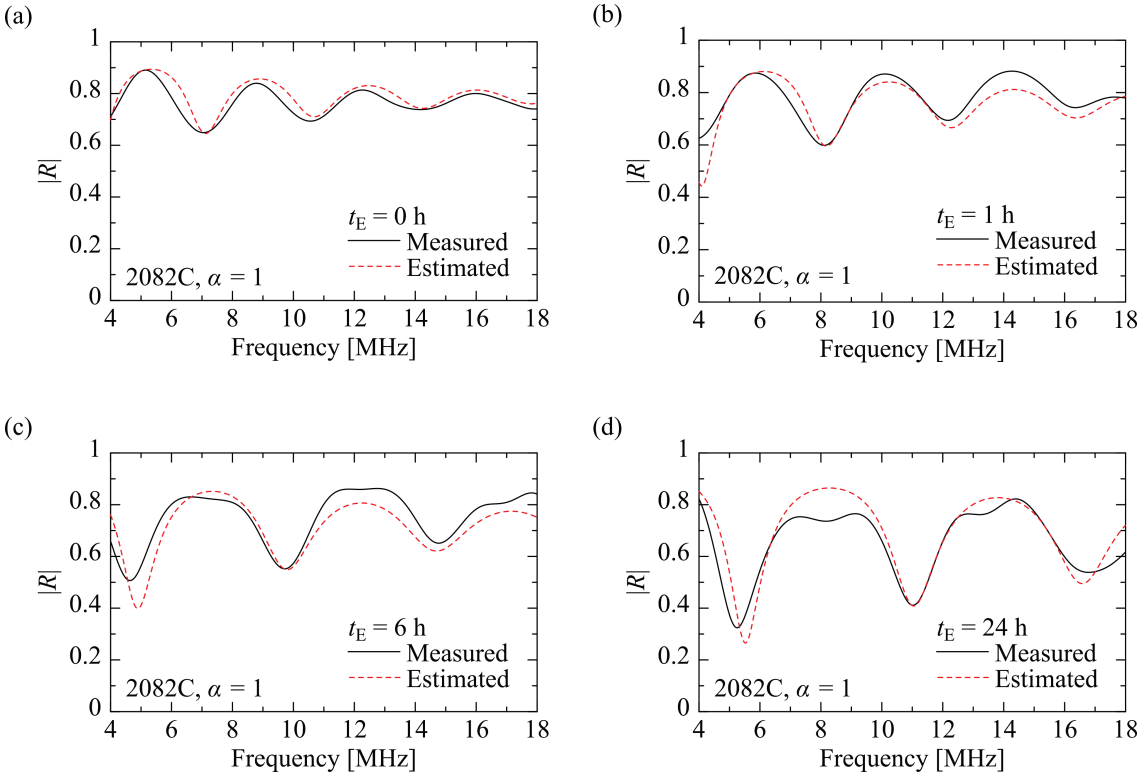

Fig. 8 Comparison of the measured and estimated reflection spectra at (a) t_E = 0, (b) t_E = 1 h, (c) t_E = 6 h, and (d) t_E = 24 h for Adhesive 1 with the mixing ratio α = 1. The theoretical estimation is based on the 2nd-order resonance characteristics.

4.2 Effects of mixing ratio

In this section, the monitoring results for Adhesive 1 with different mixing ratios α are presented following the procedures shown in Section 4.1. The ultrasonic measurements were performed for three cases of α = 1, 1/2, and 1/3, and the resonance frequencies and local minima were extracted as functions of the elapsed time t_E. Table 2 give the resonance frequencies f_m measured at the initial and final elapsed times for the mixing ratios α = 1, 1/2, and 1/3, respectively. Each resonance frequency tends to increase from t_E = 0 to t_E = 24 h, but its frequency range is different depending on the bonding condition and the resonance order m. Since viscoelastic materials such as polymers show frequency-dependent nature, not only the mixing ratio α but also the frequency would affect the estimated results of the material properties. In the present

measurement, the resonance frequency f_1 for the mixing ratio $\alpha = 1$ is much lower than the other cases. Thus, this branch is not further considered in the present section.

Table 2 Resonance frequencies f_m measured for Adhesive 1 (2082C) with different mixing ratios $\alpha = 1$, 1/2, and 1/3 at the initial and final elapsed times.

Mixing ratio α	Order m	f_m at $t_E = 0$	f_m at $t_E = 24$ h
1	1	3.28 MHz	5.23 MHz
1	2	7.06 MHz	11.02 MHz
1	3	10.57 MHz	16.75 MHz
1/2	1	5.26 MHz	8.13 MHz
1/2	2	11.14 MHz	16.44 MHz
1/3	1	4.92 MHz	7.13 MHz
1/3	2	10.22 MHz	14.34 MHz

Based on the variation of the measured resonance frequencies and local minima with the elapsed time t_E, the wave velocities and loss factors were estimated for the three mixing ratios α. Fig. 9(a) and (b) show the comparison of the wave velocity and loss factor, respectively. To illustrate the tendencies, each line in the two figures represents the moving average of neighboring five points. In Fig. 9(a), the variation of the wave velocities at the mixing ratio of $\alpha = 1$ estimated from the resonance frequencies f_2 and f_3 are almost identical. For $\alpha = 1/2$ and $\alpha = 1/3$, the wave velocities estimated by f_1 and f_2 are slightly different at the initial elapsed time, implying frequency dependence. However, it becomes less significant as the elapsed time t_E increases. At the final curing period of $t_E = 24$ h, the wave velocities at $\alpha = 1$ and $\alpha = 1/2$ are approximately 2.6 km/s, which is higher than the one at $\alpha = 1/3$, i.e., 2.2 km/s. This difference appears probably because at $\alpha = 1/3$, most part of the main agent remained due to the shortage of the curing agent.

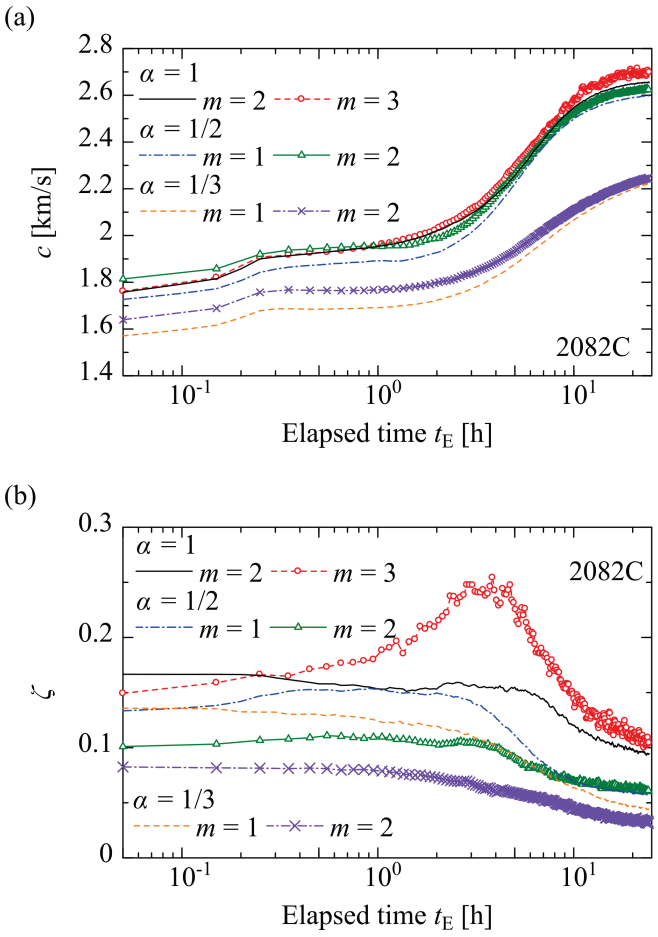

Fig. 9 Variation of (a) the wave velocities and (b) the loss factors with the elapsed time, estimated for Adhesive 1 at the mixing ratios $\alpha = 1$, 1/2, and 1/3 using two resonance modes. The data represent the moving averages of neighboring five points.

Fig. 9(b) shows the variation of the loss factors for the three mixing ratios α. Compared to the wave velocities shown in Fig. 9(a), the effect of the resonance mode order on the loss factor is significant in the curing state, e.g., $t_E < 10$ h. This implies that the loss factor depends on frequency. Furthermore, the loss factors for $(\alpha, m) = (1, 3)$ and $(\alpha, m) = (1/2, 1)$ take local maxima at around $t_E = 4$ h and 1 h, respectively, but those at $\alpha = 1/3$ decrease monotonically as the curing proceeds.

To further examine the effects of the mixing ratio, the wave velocities estimated for a single resonance order are extracted for each mixing ratio, as shown in Fig. 10(a). It is noted that the resonance orders m shown in this figure had relatively close resonance frequencies, as given in Table 2.The lines in Fig. 10(a) represent the moving averages of neighboring five points, and the error bars correspond to the standard deviations. The pot life of the adhesive at the mixing ratio of $\alpha = 1$, t_p, is shown as a reference in Fig. 10(a). The deviations of the estimated wave velocities

become sufficiently small after t_E = 0.3 h, and then the wave velocities begin to increase more rapidly after the pot life, i.e., $t_E > t_p$ = 70 min ≈ 1.17 h.

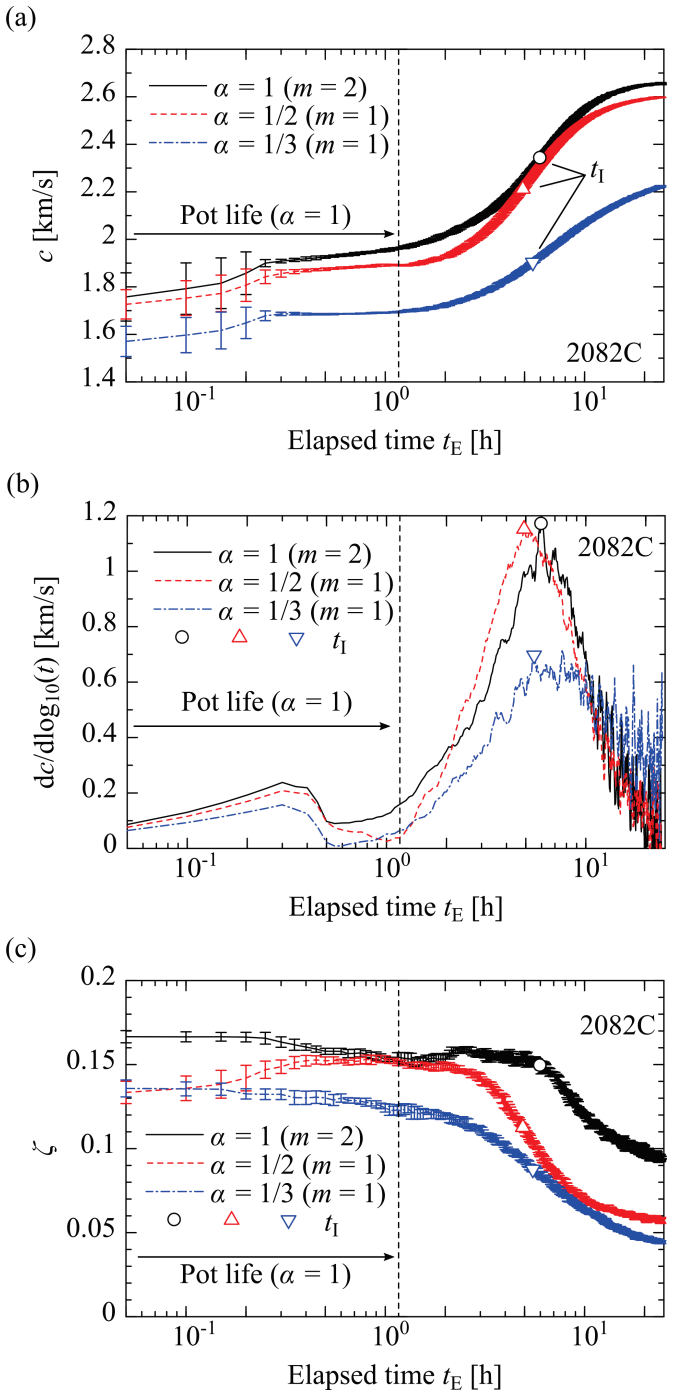

Fig. 10 Variation of (a) the wave velocities, (b) the slopes of the wave velocities, and (c) the loss factors with the elapsed time, obtained for Adhesive 1 at the mixing ratios α = 1, 1/2, and 1/3. In (a) and (c), the lines represent the moving averages of neighboring five points,

and the error bars correspond to their standard deviations. The lines in (b) represent the moving averages of neighboring eleven points.

It has been described that the wave velocities for $\alpha = 1$ and $\alpha = 1/2$ at $t_E = 24$ h are higher than that for $\alpha = 1/3$ when showing Fig. 9(a). Additionally, several differences among the three cases can be found in $t_E < 24$ h. Firstly, the slope of the wave velocity for the mixing ratio of $\alpha = 1$ before the pot life $t_E = t_p$ is steeper than the other two cases of $\alpha = 1/2$ and $\alpha = 1/3$. This feature can be confirmed more explicitly in Fig. 10(b), which shows the slopes of the wave velocities in Fig. 10(a), i.e., $dc/d\log_{10}(t)$. It is noted that the lines in Fig. 10(b) correspond to the moving averages of neighboring eleven points to suppress the effects of fluctuations. The difference between the appropriate ($\alpha = 1$) and inappropriate ($\alpha = 1/2$ and $\alpha = 1/3$) mixing ratios is distinct particularly in 0.5 h $< t_E < t_p$, where $dc/d\log_{10}(t) > 0.1$ km/s for $\alpha = 1$ but $dc/d\log_{10}(t) < 0.1$ km/s for $\alpha = 1/2$ and $\alpha = 1/3$. This result implies that the initial curing process at the appropriate mixing ratio $\alpha = 1$ is faster than inappropriate cases of $\alpha = 1/2$ and $\alpha = 1/3$.

Another interesting feature appears at the maxima of the slopes in the wave velocities. The elapsed time at which the slope of the wave velocity takes a maximum, denoted as t_I, was extracted for each mixing ratio in Fig. 10(b) and plotted together in Fig. 10(a). It is found that the slope of the wave velocity takes a maximum at around approximately $t_I = 5$ h, which is almost unchanged if the mixing ratio α is different. The mixing ratio affects the wave velocity of the adhesive at the final curing period $t_E = 24$ h, but its effect on the velocity acceleration point appears to be insignificant.

For the same set of the mixing ratio α and the resonance order m as Fig. 10(a) and (b), the estimated loss factors are shown and compared in Fig. 10(c). In this figure, the lines represent the moving averages of neighboring five points, and the error bars correspond to the standard deviations. At $\alpha = 1$, the loss factor does not rapidly change soon after the pot life t_p. However, it shows a broad peak around at $t_E = 3$ h and begins to decrease at around the velocity acceleration point $t_E = t_I$. On the other hand, the loss factors estimated for $\alpha = 1/2$ and $\alpha = 1/3$ already show decreasing behavior at $t_E = t_I$, which is rather close to the maximum change point of the loss factor. Matsukawa and Nagai [15] investigated the effects of the mixing ratio in the epoxy resin system on the variation of the wave velocity and attenuation coefficient. They discussed the measured ultrasonic properties with the glass transition temperatures, showing that the attenuation peaks resulted from the primary relaxation (α relaxation) of the resin. Their results cannot be directly compared to the ones in this section since the epoxy system and the curing conditions are different. However, the manner of the discussions in Ref. [15] might extract deeper knowledge from the measured data in the present study.

4.3 Effects of curing temperature

In this section, the effects of temperature on adhesive curing are investigated for Adhesive 2. Fig. 11(a) and (b) show the variation of the resonance frequencies f_m and local minima $|R_m|$, respectively, measured under a temperature of T = 30 °C. The changes in the resonance frequencies and local minima become almost flat around at the elapsed time t_E = 5 h. Based on the measured data, the wave velocities and loss factors are estimated for the curing adhesive, as shown in Fig. 11(c) and (d), respectively. The lines in Fig. 11(c) and (d) represent the moving averages of neighboring five points. In Fig. 11(c), the estimated wave velocities begin to increase around at the elapsed time of t_E = 0.1 h, which is earlier than those of Adhesive 1 shown in Fig. 7(a). The loss factors shown in Fig. 11(d) take local maxima at around t_E = 0.3–1 h.

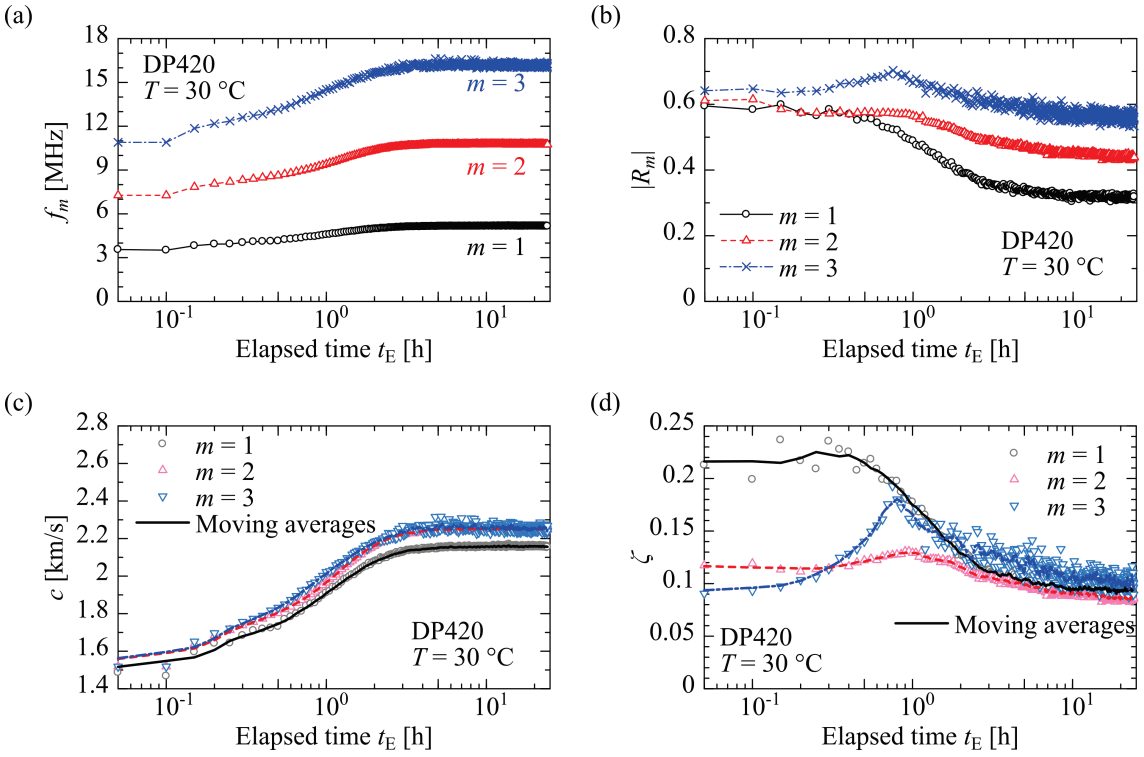

Fig. 11 Variation of (a) the resonance frequencies f_m and (b) the local minima $|R_m|$ with the elapsed time t_E, obtained for Adhesive 2 (DP420) at the temperature of T = 30 °C. (c) and (d) show the wave velocities and the loss factors estimated from the resonance frequencies and local minima at the orders m = 1, 2, and 3, respectively. The lines in (c) and (d) represent the moving averages of neighboring five points.

Similarly, the monitoring of the ultrasonic spectra was carried out for the curing of Adhesive 2 at temperatures T = 20 °C and 40 °C. Table 3 gives the resonance frequencies measured at the initial and final elapsed times under the three different curing temperatures. It is noted that the

measurement for the curing temperature T = 40 ℃ was terminated at the elapsed time t_E = 10 h because the curing progressed faster. Similarly to Table 2 for Adhesive 1, each resonance frequency in Table 3 tends to increase with increasing elapsed time t_E, and its frequency range is different depending on the bonding condition and the resonance order m. To examine the effects of the curing temperature and reduce the frequency dependence, two resonance branches were chosen for T = 30 ℃ and 40 ℃, respectively. Namely, the resonance frequencies and local minima for (m, T) = (2, 30 ℃), (3, 30 ℃), (3, 40 ℃), and (4, 40 ℃) are further considered, together with the results for (m, T) = (2, 20 ℃) and (3, 20 ℃).

Table 3 Resonance frequencies f_m measured at the initial and final elapsed times for Adhesive 2 (DP420) under different curing temperatures T = 20 ℃, 30 ℃, and 40 ℃. The final state for T = 20 ℃ and 30 ℃ corresponds to the elapsed time t_E = 24 h, while that for T = 40 ℃ represents t_E = 10 h.

Curing temperature T	Order m	f_m at t_E = 0	f_m at final state
20 ℃	2	5.87 MHz	8.93 MHz
20 ℃	3	9.00 MHz	13.50 MHz
30 ℃	1	3.55 MHz	5.15 MHz
30 ℃	2	7.25 MHz	10.76 MHz
30 ℃	3	10.91 MHz	16.29 MHz
40 ℃	2	5.96 MHz	7.02 MHz
40 ℃	3	9.04 MHz	11.10 MHz
40 ℃	4	12.05 MHz	14.41 MHz

Based on the resonance frequencies and local minima, the variation of the wave velocities and loss factors were estimated for the curing of Adhesive 2 at different temperatures, as shown in Fig. 12(a) and (b), respectively. Fig. 12(a) shows that the estimated wave velocity for T = 20 ℃ becomes almost invariant by the elapsed time t_E = 24 h, which is slower than the cases for the higher temperature, T = 30 ℃ and 40 ℃. Furthermore, the wave velocity of Adhesive 2 tends to become low with increasing curing temperature. The dependence of the wave velocity in polymer materials was reported in many previous papers [13], [17], [18], but its tendency depends on the materials. For each curing temperature T, the wave velocity was estimated by two different-order resonance frequencies, but the frequency dependence was not significant.

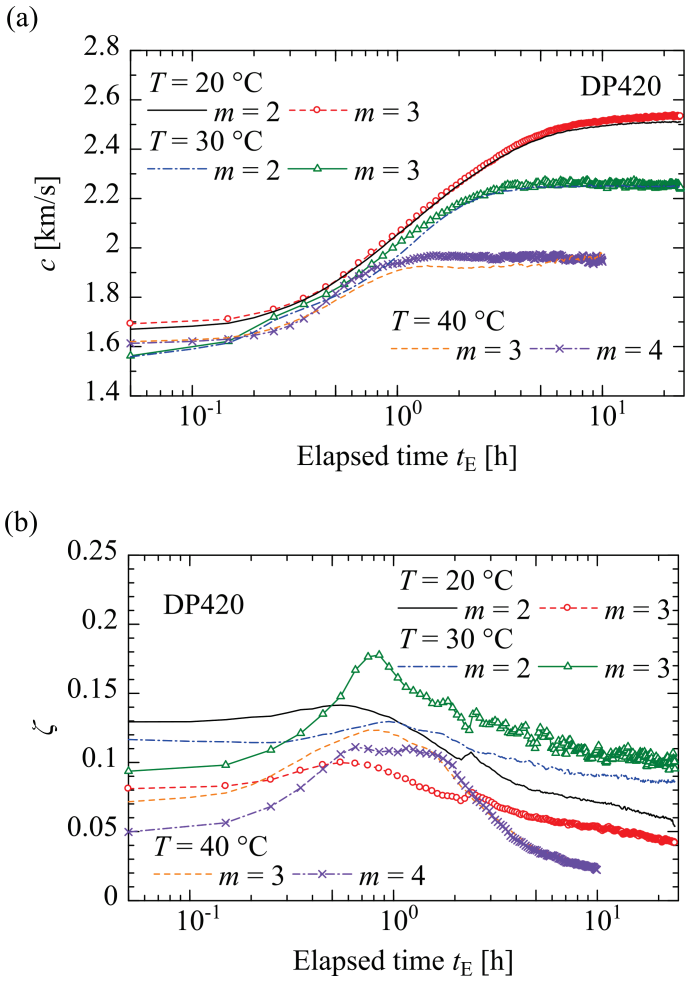

Fig. 12 Variation of (a) the wave velocities and (b) the loss factors with the elapsed time, estimated for Adhesive 2 under the curing temperatures T = 20 °C, 30 °C, and 40 °C using two resonance modes. The data represent the moving averages of neighboring five points.

The loss factors in Fig. 12(b) show different features depending on the curing temperature T and the mode order m of the resonance. At T = 20 °C, the loss factor gradually increases and begins to decrease at around t_E = 0.6 h. On the other hand, the change in the loss factor for T = 40 °C is faster than that for T = 20 °C, showing a maximum at around t_E = 0.8 h. The difference between the loss factors estimated by two resonance orders under the same curing temperature is significant compared to the wave velocities shown in Fig. 12(a). This result implies that the frequency dependence of the loss factor of Adhesive 2 is more distinct than that of the wave velocity.

To further examine the curing behavior of Adhesive 2, the wave velocities estimated for a single resonance order were extracted for each curing temperature T, as shown in Fig. 13(a). It is noted that the resonance orders m shown in Fig. 13(a) had relatively close resonance frequencies,

as given in Table 3. The pot life of the adhesive t_p = 20 min = 1/3 h at a temperature of T = 24 ℃, given in Table 1, is shown as a reference in Fig. 13(a). To specify the variations of the wave velocity, the slopes of the wave velocities in Fig. 13(a), i.e., $dc/d\log_{10}(t)$, are shown in Fig. 13(b). It is noted that the lines in Fig. 13(b) correspond to the moving averages of neighboring eleven points to suppress the effects of fluctuations. After starting the ultrasonic measurement, the slopes of the wave velocity increase monotonically. When T = 40 ℃, the slope takes a maximum around at t_E = 0.5 h, while the maxima appear around at t_E = 1 h when T = 20 ℃ and T = 30 ℃. Namely, the curing temperature does not greatly affect the peak times of the slope. This behavior is analogous to the effect of the mixing ratio, as shown in Fig. 10(b). These peak times are plotted together in Fig. 13(a).

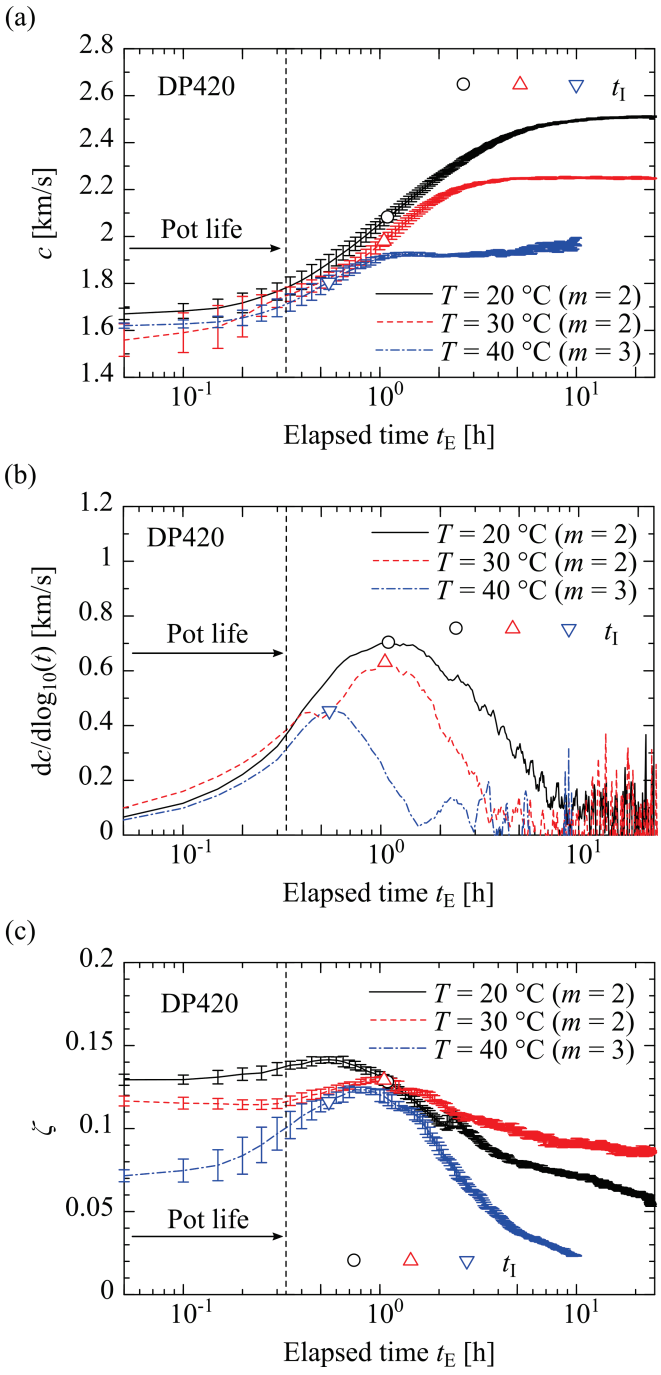

Fig. 13 Variation of (a) the wave velocities, (b) their gradients, and (c) the loss factors with the elapsed time, obtained for Adhesive 2 under the curing temperatures T = 20 ℃, 30 ℃, and 40 ℃. In (a) and (c), the lines represent the moving averages of neighboring five points, and the error bars correspond to their standard deviations. The lines in (b) represent the moving averages of neighboring eleven points. The pot life corresponds to the data at T = 24 ℃ extracted from Table 1.

The comparison of the loss factors estimated for the three different curing temperatures is shown in Fig. 13(c). At the beginning of the curing process, the loss factor of the adhesive tends to be low when the curing temperature T is low. The slopes of the loss factors for the curing temperatures of T = 20 ℃ and 30 ℃ begin to increase at around the pot life. The difference of the elapsed times when the loss factor takes a maximum is not distinct among the curing temperatures, but the variation of the loss factor at T = 20 ℃ and 30 ℃ is broader than that at T = 40 ℃. Freemantle and Challis [16] reported a similar behavior of the ultrasonic attenuation coefficient peak due to the change in the curing temperature. They inferred that the attenuation coefficient has a peak earlier under high curing temperatures because the molecular chains and the cross-linking are rapidly developed. Similar phenomena would appear in the results of the present study.

5. Concluding remarks

In this paper, a curing monitoring technique has been proposed for an adhesive layer between metal plates, based on the ultrasonic resonance phenomenon. Adhesive bonds have been modeled as a viscoelastic material that is characterized by wave velocity and loss factor, and the ultrasonic propagation behavior has been theoretically analyzed for a trilayer structure subjected to the normal wave incidence. The theoretical analysis has shown that the resonance characteristics in the reflection spectrum enable it to estimate the wave velocity and loss factor of the adhesive layer. Based on this result, ultrasonic monitoring has been performed for the curing of bi-component epoxy adhesives. The estimated wave velocities tend to increase in the curing process, while the loss factors show different behavior depending on the bonding condition and the frequency. If the mixing ratio of the curing and main agents has been imbalanced, the wave velocity and loss factor have varied gradually. However, the elapsed time when the maximum slope of the wave velocity appears after applying the adhesive has not been significantly affected by the mixing ratio. The local maximum of the estimated loss factor has disappeared if the mixing ratio is low. Furthermore, the increase in the curing temperature has promoted the curing reaction, making the changes in the wave velocity and loss factor faster. The estimated wave velocities have shown temperature dependence. The variation of the estimated loss factors has also depended on the curing temperature, but their peak times have been almost invariant. The combination of the proposed technique in this study with other measurement methods and theories, such as the glass transition temperature measurement and the relaxation theory, would help to understand the curing behavior of adhesives more deeply.

Acknowledgement

This study has been supported by Grants-in-Aid for Scientific Research (KAKENHI) Grant No. 23K03590 from Japan Society for the Promotion of Science (JSPS).

References

[1] Guyott C C H and Cawley P 1988 Evaluation of the cohesive properties of adhesive joints using ultrasonic spectroscopy NDT International 21 233–40

[2] Wang W and Rokhlin S I 1991 Evaluation of interfacial properties in adhesive joints of aluminum alloys using angle-beam ultrasonic spectroscopy J. Adhes. Sci. Technol. 5 647–66

[3] Koodalil D, Rajagopal P and Balasubramaniam K 2021 Bond stiffness estimation with shear horizontal guided waves generated using PPM-EMATs Int. J. Adhes. Adhes. 104 102761

[4] Mori N, Wakabayashi D and Hayashi T 2022 Tangential bond stiffness evaluation of adhesive lap joints by spectral interference of the low-frequency A0 lamb wave Int. J. Adhes. Adhes. 113 103071

[5] Li Y, Lyu Y, Wu B, Gao J, Bian Z and He C 2023 Experimental investigation of bonding quality for CFRP bonded structures with thick adhesive layers based on ultrasonic transmission coefficient spectrums J. Nondestr. Eval. 43 17

[6] Dietz A G H, Hauser E A, McGarry F J and Sofer G A 1956 Ultrasonic waves as a measure of cure Ind. Eng. Chem. 48 75–75

[7] Papadakis E P 1974 Monitoring the moduli of polymers with ultrasound J. Appl. Phys. 45 1218–22

[8] Lindrose A M 1978 Ultrasonic wave and moduli changes in a curing epoxy resin Exp. Mech. 18 227–32

[9] Dixon S, Jaques D and Palmer S B 2003 The development of shear and compression elastic moduli in curing epoxy adhesives measured using non-contact ultrasonic transducers J. Phys. D Appl. Phys. 36 753–59

[10] Aggelis D G and Paipetis A S 2012 Monitoring of resin curing and hardening by ultrasound Construction and Building Materials 26 755–60

[11] Zhang Y, Wang X, Yang Q, Xue R, Zhang J, Sun Y, Xu D and Krishnaswamy S 2020 Research on epoxy resin curing monitoring using laser ultrasonic Measurement 158 107737

[12] Rokhlin S I, Lewis D K, Graff K F and Adler L 1986 Real-time study of frequency dependence of attenuation and velocity of ultrasonic waves during the curing reaction of epoxy resin J. Acoust. Soc. Am. 79 1786–93

[13] Alig I, Lellinger D, Nancke K, Rizos A and Fytas G 1992 Dynamic light scattering and ultrasonic investigations during the cure reaction of an epoxy resin J. Appl. Polym. Sci. 44 829–35

[14] Nguyen N T, Lethiecq M and Gerard J F 1995 Glass transition characterization of homogeneous and heterogeneous polymers by an ultrasonic method Ultrasonics 33 323–9

[15] Matsukawa M and Nagai I 1996 Ultrasonic characterization of a polymerizing epoxy resin with imbalanced stoichiometry J. Acoust. Soc. Am. 99 2110–5

[16] Freemantle R J and Challis R E 1998 Combined compression and shear wave ultrasonic measurements on curing adhesive Meas. Sci. Technol. 9 1291–302

[17] Lionetto F and Maffezzoli A 2005 Relaxations during the postcure of unsaturated polyester networks by ultrasonic wave propagation, dynamic mechanical analysis, and dielectric analysis J. Polym. Sci. B Polym. Phys. 43 596–602

[18] Lionetto F and Maffezzoli A 2009 Polymer characterization by ultrasonic wave propagation Adv. Polym. Technol. 27 63–73

[19] Ghodhbani N, Maréchal P and Duflo H 2016 Ultrasound monitoring of the cure kinetics of an epoxy resin: Identification, frequency and temperature dependence Polym. Test. 56 156–66

[20] Adachi T, Ishii Y, Hirota K and Tanabe D 2023 Ultrasonic monitoring of adhesive curing process between adherends Int. J. Adhes. Adhes. 103363

[21] Fraisse P, Schmit F and Zarembowitch A 1992 Ultrasonic inspection of very thin adhesive layers J. Appl. Phys. 72 3264–71

[22] Mori N, Matsuda N and Kusaka T 2019 Effect of interfacial adhesion on the ultrasonic interaction with adhesive joints: A theoretical study using spring-type interfaces J. Acoust. Soc. Am. 145 3541–50

[23] Mori N, Iwata Y, Hayashi T and Matsuda N 2023 Viscoelastic wave propagation and resonance in a metal–plastic bonded laminate Mech. Adv. Mater. Struct. 30 3803–16

[24] Pialucha T and Cawley P 1994 The detection of thin embedded layers using normal incidence ultrasound Ultrasonics 32 431–40

[25] Mori N and Hayashi T 2023 Ultrasonic interference and critical attenuation in metal-plastic bilayer laminates J. Sound Vib. 547 117531